

## Synthesis and Stabilization of FeCo Nanoparticles

Girija S. Chaubey,<sup>#</sup> Carlos Barcena,<sup>‡</sup> Narayan Poudyal,<sup>#</sup> Chuanbing Rong,<sup>#</sup> Jinming Gao,<sup>‡</sup>  
Shouheng Sun,<sup>§</sup> and J. Ping. Liu<sup>\*,#</sup>

Department of Physics, University of Texas at Arlington, Arlington, Texas 76019, Simmons Comprehensive Cancer Center, University of Texas Southwestern Medical Center at Dallas, Dallas, Texas 75390, and Department of Chemistry, Brown University, Providence, Rhode Island 02916

Received February 7, 2007; E-mail: pliu@uta.edu

FeCo alloys are an important soft magnetic material because of their unique magnetic properties including large permeability and very high saturation magnetization. FeCo nanoparticles are ideal building blocks for nanostructured thin film or bulk magnetic materials<sup>1–3</sup> and are also suitable for biomedical applications.<sup>4</sup> However, synthesis of monodisperse FeCo nanoparticles remains a challenging task due to the poor chemical stability of the nanoparticles. Several attempts to synthesize FeCo nanoparticles have been made to obtain particles with desired size and composition.<sup>5–8</sup> Desvaux et al.<sup>9</sup> synthesized FeCo nanoparticles by co-decomposition of organometallic precursors under hydrogen. Superlattice multilayers of the FeCo nanoparticles were successfully obtained. Recently, Seo et al. have obtained FeCo/graphite core/shell nanocrystals by chemical vapor deposition method and investigated their applications in magnetic resonance imaging *in vivo*.<sup>10</sup>

In this paper, we report a simple method to synthesize bimetallic FeCo nanoparticles with well-controlled particle size and size distribution.<sup>11</sup> The synthesis is based on reductive decomposition of Fe(III) acetylacetonate (Fe(acac)<sub>3</sub>) and Co(II) acetylacetonate (Co(acac)<sub>2</sub>) in a mixture of surfactants and 1,2-hexadecanediol (HDD) under a gas mixture of 93% Ar + 7% H<sub>2</sub> at 300 °C. X-ray diffraction (XRD) measurements showed that FeCo nanoparticles could also be synthesized under argon atmosphere, indicating that HDD was the reducing agent in the reaction. However, partial oxidation was observed from the samples synthesized in argon, which means that the presence of a fraction of hydrogen played an important role in protecting the particles from oxidation.

Size of the nanoparticles can be well-controlled by varying the binding ligands. FeCo nanoparticles of average 20 nm size were obtained when a mixture of oleic acid and oleyl amine was used as surfactant. Using oleyl amine alone could also produce FeCo nanoparticles, but the shape of the particles was difficult to control and the particles were prone to aggregate in the dispersion. Similarly, particles with an average size of 10 nm with narrow size distribution (SD = 12%) were obtained by using a combination of oleic acid and trioctylphosphine (TOP) as surfactants (Supporting Information).

Figure 1A shows the transmission electron microscopy (TEM) image of the FeCo particles with average diameter of 20 nm. Analysis on the TEM images indicates that the nanoparticles are monodisperse with narrow size distributions (SD = 7%). XRD patterns of the as-synthesized samples (Figure 1B) show typical bcc structure of the FeCo alloy phase, indicating crystal nature of the nanoparticles. The average particle diameter estimated from the XRD using the Scherrer equation<sup>12</sup> was 19 nm, which is very close to the size determined by statistical analysis of the TEM images.

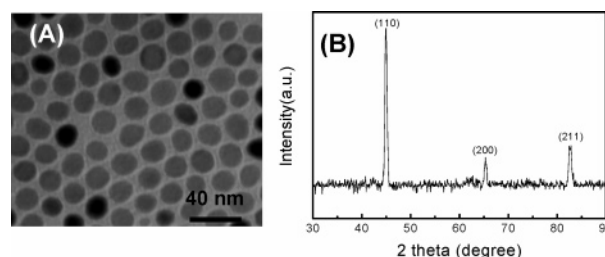


**Figure 1.** (A) TEM bright-field image of the FeCo nanoparticles and (B) X-ray diffraction patterns of the as-synthesized 20 nm FeCo nanoparticles.

The chemical stability of the FeCo nanoparticles in air is dependent on the nature of the binding ability of the surfactants as well as their chemical compositions. Due to their oxophilicity, oleic acid and TOP tend to form a stronger chemical bond with the nanoparticles than oleyl amine. As a result, the 10 nm FeCo nanoparticles, which were bonded by oleic acid and TOP, were found to be chemically more stable than the 20 nm FeCo particles. The chemical stability of the FeCo nanoparticles in air is also dependent on the chemical compositions of the particles. For both 10 and 20 nm particles, the Fe/Co ratio was controlled by varying the initial molar ratio of the metal precursors. For example, FeCo nanoparticles of atomic percentage 60 to 40 for Fe to Co were obtained by feeding an initial molar ratio of 1.5:1 for Fe and Co metal precursors, whereas atomic percentage 50 to 50 for Fe to Co was obtained when an initial feeding molar ratio was 1:1 for Fe to Co metal precursors. The final particle composition was confirmed by EDX. It was found that air stability of the FeCo nanoparticles with equal composition of Fe and Co was much higher compared to the Fe-rich nanoparticle. It can be clearly seen from the XRD patterns of 20 nm FeCo (Supporting Information) that, when the initial molar ratio of Fe/Co metal precursors is 1, only pure FeCo phase can be formed whereas an increase in Fe content resulted in slight oxidation of FeCo. All of the XRD measurements were made within 2 h of particle synthesis, and all samples were handled under air atmosphere. Similar results were obtained in the case of 10 nm particles, as well.

It is hard to wash out the surfactants completely from the surface of as-synthesized nanoparticles. The presence of surfactants on the surface of nanoparticles causes difficulty in determining actual magnetization value. In order to determine the actual magnetization of the particles, atomic absorption spectroscopy (AAS) was used to quantitatively determine the content of Fe/Co metals and surfactants in the nanoparticles (Supporting Information). An AAS experiment was carried out on FeCo nanoparticles having a Fe/Co ratio of 1.5. The nanoparticles were initially washed four times with hexane and ethanol mixture. The AAS result showed that the presence of surfactants on the surface of nanoparticles contributed

<sup>#</sup> University of Texas at Arlington.

<sup>‡</sup> University of Texas Southwestern Medical Center at Dallas.

<sup>§</sup> Brown University.

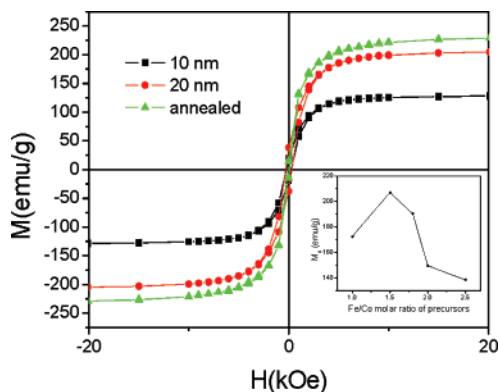


**Figure 2.** Room-temperature hysteresis loops of FeCo nanoparticles annealed at 500 °C under Ar (93%) + H<sub>2</sub> (7%), for 30 min, and the 10 and 20 nm as-synthesized FeCo nanoparticles. The inset shows variation of magnetization with different molar ratio of Fe/Co metal precursors for the 20 nm FeCo particles.

22.1% weight of the FeCo nanoparticle samples, and we used this result to calibrate the magnetization values measured directly from the samples.

Magnetic properties of these particles are size dependent. The saturation magnetizations ( $M_s$ ) of 207 and 129 emu/g were obtained for 20 and 10 nm FeCo particles (Figure 2). Hysteresis measurements show that the as-synthesized nanoparticles are ferromagnetic at room temperature with coercivity around 300 Oe. Magnetic properties of the FeCo nanoparticles are also composition dependent. Maximum magnetization was obtained for FeCo with an Fe/Co ratio of 1.5, which is consistent with that for the bulk FeCo alloy.<sup>3</sup> An increase or decrease of Fe/Co molar ratio resulted in a decrease in the magnetization value. A graph showing  $M_s$  versus Fe/Co molar ratio for the 20 nm FeCo particle is shown in the inset of Figure 2. In addition to size and composition effects, refluxing temperature during the synthesis also plays an important role in determining  $M_s$ . It was observed that, when the reaction mixture was refluxed at 290 °C, the  $M_s$  values for 10 and 20 nm FeCo were 122 and 171 emu/g, respectively. On the other hand, by raising the refluxing temperature to 300 °C, the  $M_s$  values for the 10 and 20 nm particles were increased to 129 and 207 emu/g. Further increase in refluxing temperature did not result in increased  $M_s$ .

The nanoparticles were found to be slowly oxidized when exposed to air, leading to the formation of an oxide shell<sup>13</sup> (Supporting Information) and a decrease in  $M_s$  of the nanoparticles. For example, exposing the particles to air for 48 h resulted in 25% decrease in  $M_s$  for the 20 nm particles and 21% decrease for the 10 nm particles (Figure S4). The difference in the magnetization decrease could be attributed to the binding ability of the surfactants, as we discussed earlier. The 10 nm particles were bonded by oleic acid and TOP; owing to their oxophilic character, these surfactants bind strongly to the nanocrystal surface, leading to the decrease in surface oxidation rate as discussed earlier. In comparison, the surface oxidation rate was higher for the 20 nm particles, which were encapsulated by oleic acid and oleyl amine. To overcome this oxidation problem, the particles were annealed at 500 °C for 30 min under a gas mixture of 93% Ar + 7% H<sub>2</sub>. Transmission electron microscopy image of the annealed 20 nm particles shows that there are no significant changes in size and shape of the particles. XRD patterns of the annealed FeCo particles show typical bcc structure (Supporting Information). Average particle diameter calculated from the XRD patterns of the annealed particles using the Scherrer formula<sup>12</sup> was 21 nm, which further supported the claim that no significant change in size occurred after annealing. However, an

annealing process has resulted in formation of a carbon shell around the surface of the particles<sup>9,14</sup> (Supporting Information). The presence of carbon in the annealed sample was determined by Raman spectroscopy (Supporting Information). It is believed that the presence of a carbon shell might have prevented the particles from sintering when annealed at 500 °C for 30 min. After the annealing, the particles became air-stable with enhanced magnetization (see Figure 2), which may be attributed to the fact that the annealing process leads to a homogeneous atomic distribution of iron and cobalt within individual nanoparticles. EDX analysis on the annealed sample shows similar compositions as their as-synthesized counterpart. Curves in Figure 2 show a dramatic increase in the  $M_s$  of the particles to  $M_s = 230$  emu/g, which is very close to the value for the bulk material ( $M_s = 245$  emu/g).

In conclusion, an alternative method for the synthesis of monodisperse FeCo nanoparticles of controlled size and magnetic properties has been developed via reductive decomposition of organometallic precursors in the presence of surfactants. Saturation magnetization of the particles is dependent on particle size. The particles can be made air-stable with enhanced magnetic properties by annealing at modest temperatures. The stabilized nanoparticles can be ideal building blocks for high-performance nanocomposite permanent magnets and nanostructured magnetic devices and can also be suitable for biomedical applications.

**Acknowledgment.** This work was supported by ONR/MURI under Grant No. N00014-05-1-0497 to J.P.L. and NIH R21 EB005394 to J.G.

**Supporting Information Available:** Typical experimental procedures of 10 and 20 nm particles, TEM image of 10 nm particles, and other supporting figures of the FeCo nanoparticles. This material is available free of charge via the Internet at <http://pubs.acs.org>.

## References

- (1) Zeng, H.; Li, J.; Liu, J. P.; Wang, Z. L.; Sun, S. *Nature* **2002**, *420*, 395–398.
- (2) Zeng, H.; Li, J.; Wang, Z. L.; Liu, J. P.; Sun, S. *Nano Lett.* **2004**, *4*, 187–190.
- (3) (a) Bozorth, R. M. *Ferromagnetism*; Van Nostrand: New York, 1951. (b) Sunder, R. S.; Deevi, S. C. *Int. Mater. Rev.* **2005**, *50*, 157–192.
- (4) (a) Behrens, S.; Bonnemann, H.; Matoussevitch, N.; Gorschinski, A.; Dinjus, E.; Habicht, W.; Bolle, J.; Zinoveva, S.; Palina, N.; Hormes, J.; Modrow, H.; Bahr, S.; Kemper, V. *J. Phys.: Condens. Matter* **2006**, *18*, S2543–S2561. (b) Gould, P. *Nanotoday* **2006**, *1*, 34–39. (c) Bai, J.; Wang, J. P. *Appl. Phys. Lett.* **2005**, *87*, 152502–152505. (d) Hutten, A.; Sudfeld, D.; Ennem, I.; Reiss, G.; Wojczykowski, K.; Jutzi, P. *J. Magn. Mater.* **2005**, *293*, 93–101.
- (5) Viau, G.; Fievet-Vicent, F.; Fievet, F. *J. Mater. Chem.* **1996**, *6*, 1047–1053.
- (6) Su, X.; Zheng, H.; Yang, Z.; Zhu, Y.; Pan, A. *J. Mater. Sci.* **2003**, *38*, 4581–4585.
- (7) Bönemann, H.; Brand, R. A.; Brijoux, W.; Hofstadt, H. W.; Frerichs, M.; Kemper, V.; Maus-Freidrichs, W.; Matoussevitch, N.; Nagabhushana, K. S.; Voigts, V.; Caps, V. *Appl. Organomet. Chem.* **2005**, *19*, 790–796.
- (8) (a) Kodama, D.; Shinoda, K.; Sato, K.; Konno, Y.; Joseyphus, R. J.; Motomiya, K.; Takahashi, H.; Matsumoto, T.; Sato, Y.; Tohji, K.; Jayadevan, B. *Adv. Mater.* **2006**, *18*, 3154–3159. (b) Kodama, D.; Shinoda, K.; Sato, K.; Sato, Y.; Jayadevan, B.; Tohji, K. *IEEE Trans. Magn.* **2006**, *42*, 2796–2798.
- (9) Desvaux, C.; Amiens, C.; Fejes, P.; Renaud, P.; Respaud, M.; Lecante, P.; Snoeck, E.; Chaudret, B. *Nat. Mater.* **2005**, *4*, 750–753.
- (10) Seo, W. S.; Lee, J. H.; Sun, Z.; Suzuki, Y.; Mann, D.; Liu, Z.; Terashima, M.; Yang, P.; McConnell, M. V.; Nishimura, D. G.; Dai, H. *Nat. Mater.* **2006**, *5*, 971–976.
- (11) The Fe source used in some previous studies was Fe(CO)<sub>5</sub>, which is a highly toxic, highly flammable liquid at room temperature. The reaction temperature is above the boiling point of 103 °C of Fe(CO)<sub>5</sub>, therefore some Fe(CO)<sub>5</sub> may be lost and it is difficult to maintain the compositions.
- (12) Cullity, B. D. *Introduction to Magnetic Materials*; Addison-Wesley: Reading, MA, 1972.
- (13) Turgut, Z.; Nuhfer, N. T.; Piehler, H. R.; McHendry, M. E. *J. Appl. Phys.* **1999**, *85*, 4406–4408.
- (14) Turgut, Z.; Huang, M.-Q.; Gallagher, K.; McHendry, M. E.; Majestic, S. A. *J. Appl. Phys.* **1997**, *81*, 4039–4041.

JA0708969